

Supplemental Information

***FOXA1* Mutations Reveal Distinct Chromatin Profiles
and Influence Therapeutic Response in Breast Cancer**

Amaia Arruabarrena-Aristorena, Jesper L.V. Maag, Srushti Kittane, Yanyan Cai, Wouter R. Karthaus, Erik Ladewig, Jane Park, Srinivasaraghavan Kannan, Lorenzo Ferrando, Emiliano Cocco, Sik Y. Ho, Daisylyn S. Tan, Mirna Sallaku, Fan Wu, Barbara Acevedo, Pier Selenica, Dara S. Ross, Matthew Witkin, Charles L. Sawyers, Jorge S. Reis-Filho, Chandra S. Verma, Ralf Jauch, Richard Koche, José Baselga, Pedram Razavi, Eneda Toska, and Maurizio Scaltriti

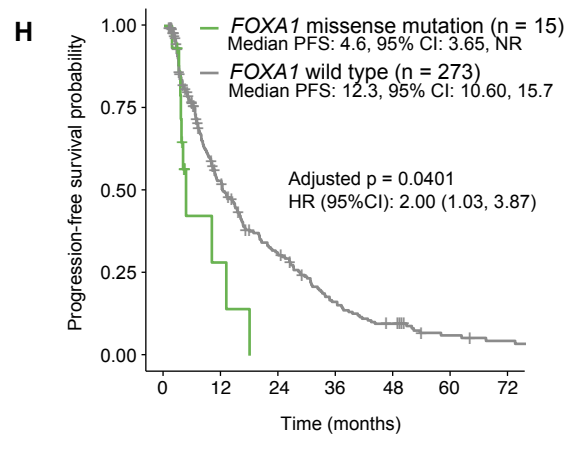
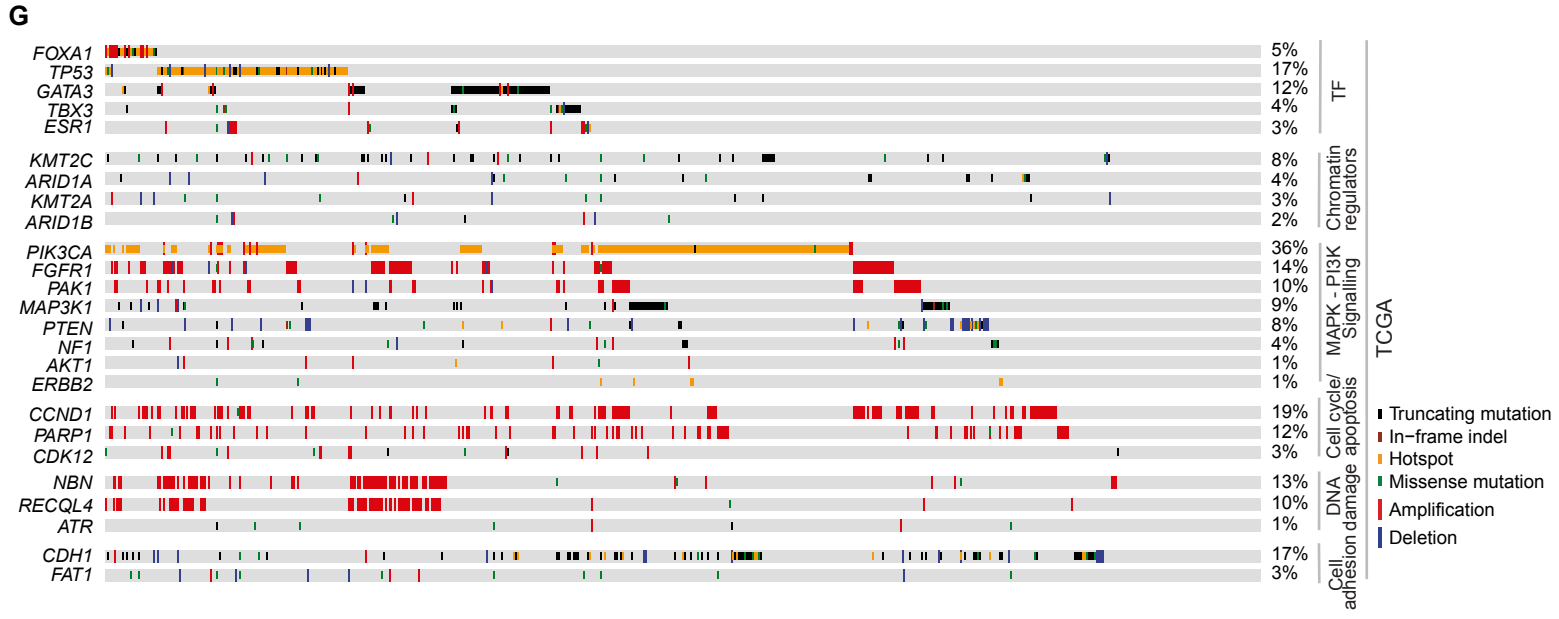
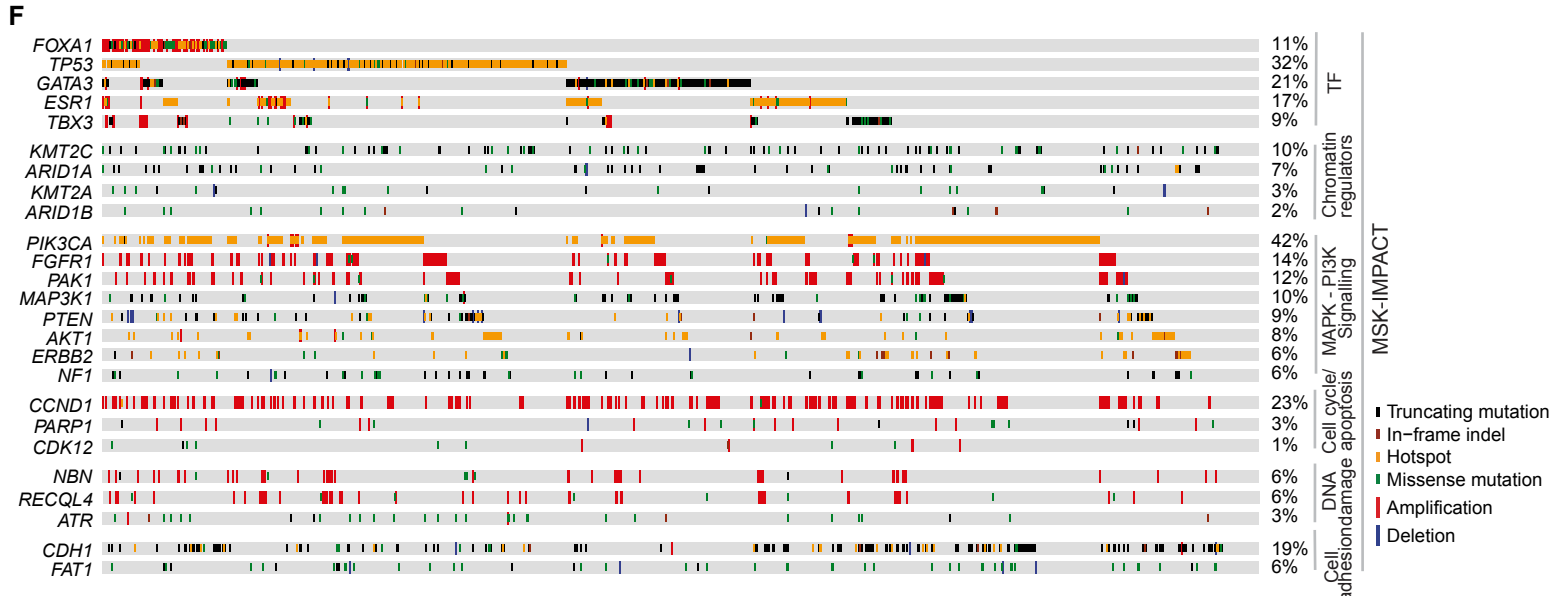
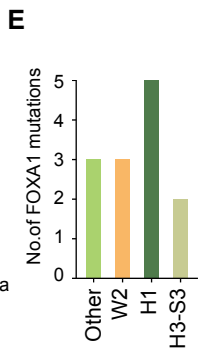
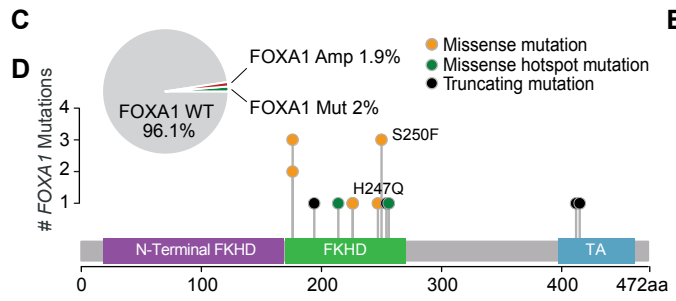
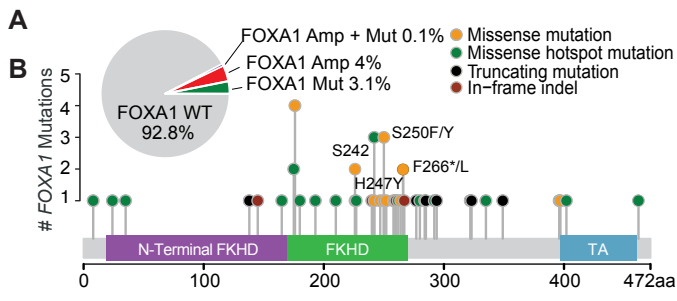


Figure S1. Related to Figure 1. *FOXA1* hotspot mutations cluster at C-terminal FKH domain and are mutually exclusive with *ESR1* mutations.

(A, C) Pie charts representing frequency of *FOXA1* alteration types (wild-type (WT), amplification (Amp), mutation (Mut) or both (Amp + Mut)) among breast cancer patients from the curated list utilized for survival analysis in Figure 1G and TCGA respectively.

(B, D) Lollipop plots depicting distribution of *FOXA1* mutations (truncating, missense and in-frame indels) found among breast cancer patients from the curated list utilized for survival analysis in Figure 1G and TCGA respectively, along the protein sequence.

(E) Bar-plot showing number of mutations per subdomains indicated, for patients in TCGA cohort. W2, Wing2; H1, Helix1; H3-S3, from helix3 to third beta strand.

(F, G) Association of full cohort of samples, including *FOXA1* mutant and wild-type (WT) samples, with pattern, frequency and type of genomic alterations of the key breast cancer genes indicated among breast cancer patients from www.cbioportal.org (F) and TCGA (G). Genes with alteration frequency > 5% were represented.

(H) Kaplan-Meier curves displaying progression-free survival of patients harboring either WT or mutant *FOXA1* under aromatase inhibitor treatment, excluding patients harboring concomitant *ESR1* mutations. P value as indicated, log rank test.

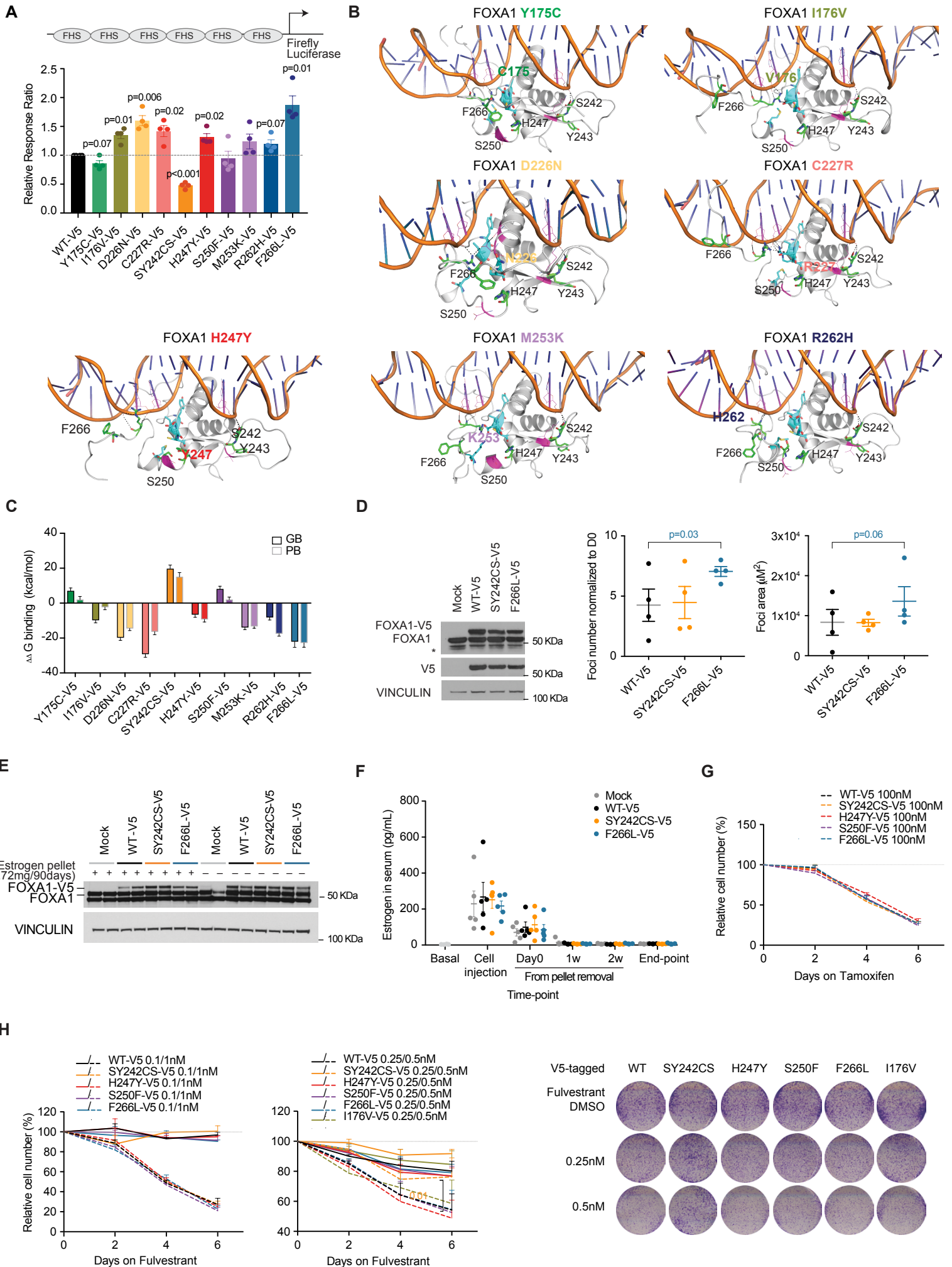


Figure S2. Related to Figure 2. FOXA1 forkhead mutations show enhanced transcriptional activity, and structural alterations.

(A) Impact of ectopic expression of V5-tagged FOXA1 variants (Y175C, I176V, D226N, C227R, SY242CS, H247Y, S250F, M253K, R262H, F266L) on luciferase reporter activity (n=4 independent experiments as indicated by dots). Two-tailed Student's t-test with Welch's T test for different variance correction, p-values as indicated. Error bars, mean \pm SEM.

(B) Impact of ectopic expression of V5-tagged FOXA1 variants (Y175C, I176V, D226N, C227R, H247Y, M253K, R262H) 3-D structural interaction of the forkhead domain (FKHD) with DNA.

(C) Impact of ectopic expression of V5-tagged FOXA1 variants (Y175C, I176V, D226N, C227R, SY242CS, H247Y, S250F, M253K, R262H, F266L) on binding free energy ($\Delta\Delta G$) calculated using the Generalized Born (GB) and Poisson-Boltzmann (PB) formalisms averaged over the conformations of the complexes sampled during atomistic Molecular Dynamics (MD) simulations.

(D) Effect of ectopic expression of FOXA1 WT-V5, SY242CS-V5, and F266L-V5 on protein abundance (left, representative experiment is shown) and foci number and area under estrogen deprivation in T47D cells (right, n=4 independent experiments as indicated by dots). *, unspecific band.

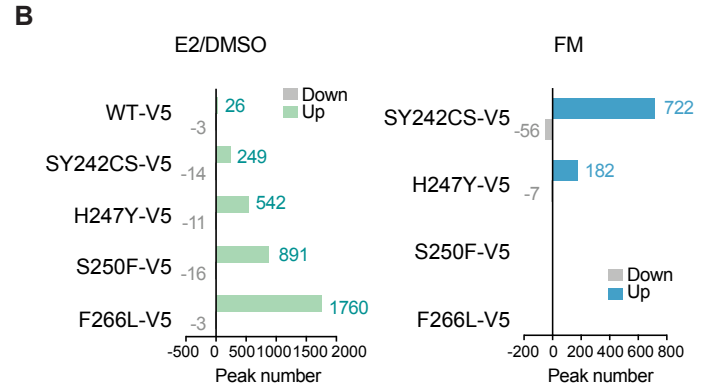
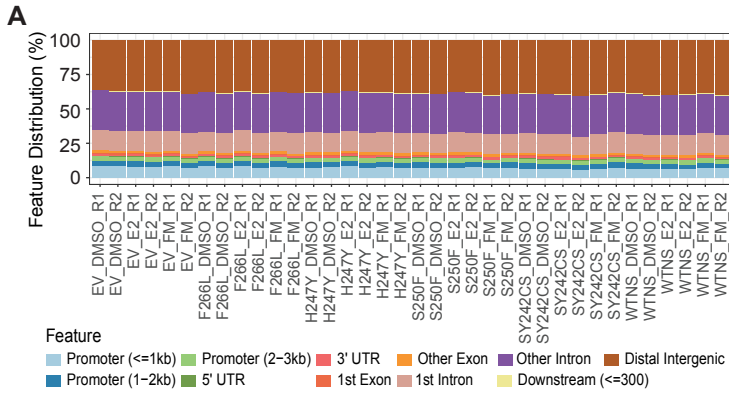
One-tailed Student's t-test, p-values as indicated.

(E) Immunoblot of depicted proteins from representative xenograft tumors of Mock or V5-tagged FOXA1 variant (WT, SY242CS and F266L) expressing MCF7 cells.

(F) Estrogen levels (pg/mL) in mice sera during indicated time-points of the *in vivo* experiment (n=4 mice for the basal group and n=5 mice for the rest).

(G) Impact of ectopic expression of V5-tagged FOXA1 variants (Y175C, I176V, D226N, C227R, SY242CS, H247Y, S250F, M253K, R262H, F266L) on cell-number upon tamoxifen treatment (100nM) *in vitro* (n=3 independent experiments). Two-tailed Student's t-test.

(H) Impact of ectopic expression of V5-tagged FOXA1 variants (Y175C, I176V, D226N, C227R, SY242CS, H247Y, S250F, M253K, R262H, F266L) on cell-number upon fulvestrant treatment (0.1 and 1nM (n=3 independent experiments), left; 0.25 and 0.5nM (n=3 independent experiments), middle; representative images of crystal violet staining upon 0.25 and 0.5nM fulvestrant treatment, right) *in vitro*. Two-tailed Student's t-test, p-values as indicated.



C

CI Top enriched <i>de novo</i> motifs	T%	BG%	p-val
1 GTAAACA FORKHEAD	65.92	14.50	1e ⁻⁵⁷⁴
CCGCCATT YY2	7.06	0.37	1e ⁻¹²²
GTCACACA SMAD	10.34	1.46	1e ⁻¹⁰⁰
2 AGTAAACA FORKHEAD	45.99	17.96	1e ⁻¹⁶¹
TCTATTCG DEAF1	2.24	0.31	1e ⁻²⁷
GTTCGGTT MYB	3.14	0.71	1e ⁻¹⁸
3 TGTTTACT FORKHEAD	72.40	29.44	1e ⁻⁴⁷⁰
ATGACTCA AP1	22.91	5.80	1e ⁻¹⁹³
AAACCGGT GRHL1	27.02	15.96	1e ⁻⁴⁸
4 TTTATTTA Alternative motif	70.08	28.23	1e ⁻⁶³¹
TGTAAACA FORKHEAD	19.36	9.24	1e ⁻⁸¹
SCCTCAGG AP2gamma	20.68	12.34	1e ⁻⁴⁷
5 TGTTTACA FORKHEAD	64.54	20.31	1e ⁻⁴²⁷
ATGACTCA AP1	29.79	11.20	1e ⁻¹¹⁸
AAACCGGT GRHL1	24.68	14.10	1e ⁻³⁷
6 AGGTCAGC NUCLEAR RECEPTOR	43.84	17.60	1e ⁻⁷⁰⁴
TGTTTAC FORKHEAD	54.28	27.38	1e ⁻¹⁵⁴
AATCAGAT GATA	18.53	10.67	1e ⁻²⁷
7 TGTAACA FORKHEAD	81.28	24.26	1e ⁻⁶³⁰
AATATTTG ARID	29.77	9.16	1e ⁻¹⁵⁰
TATCIGAT GATA	9.91	4.63	1e ⁻²²

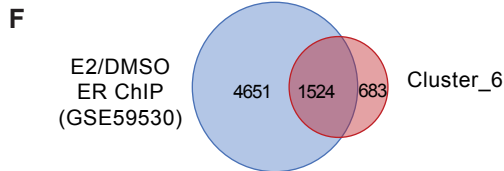
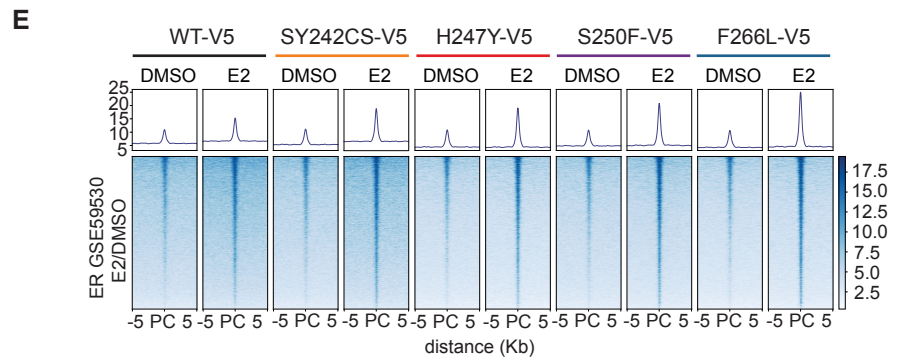
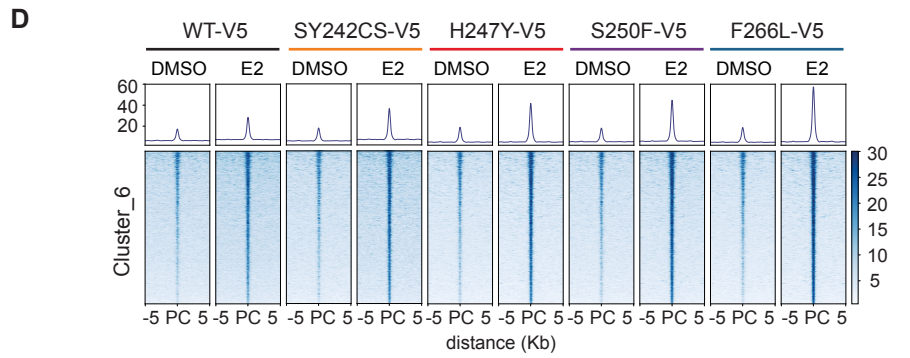


Figure S3. Related to Figure 3. *FOXA1* Wing2 mutations show enhanced affinity for ER loci and ER-mediated transcription

(A) Stacked bar plot depicting genomic feature distribution per ChIP-seq sample (n=2 biological replicates).

(B) Bar plots representing number of differential peaks for *FOXA1* mutant (SY242CS-V5, H247Y-V5, S250F-V5 and F266L-V5) and control (WT-V5, wild-type) MCF7 cells upon estrogen stimulation (left panel) and differential peaks for *FOXA1* mutant (SY242CS-V5, H247Y-V5, S250F-V5 and F266L-V5) as compared to *FOXA1* WT in full-media (FM, right panel).

(C) Table depicting top enriched Homer *de novo* motifs and the transcription factors associated with, per ChIP-seq cluster indicated. Fisher's exact test, p-value (p-val) as indicated. T%, percentage of target sites; BG%, background percentage; Cl, cluster.

(D) Tornado plot representing *FOXA1* binding peaks at cluster 6 in the absence (DMSO) or presence of estrogen (E2) in *FOXA1* mutant (SY242CS-V5, H247Y-V5, S250F-V5 and F266L-V5) and WT-V5 MCF7 cells. PC, Peak center. Average of 2 biological replicates is represented.

(E) Tornado plot representing *FOXA1* binding peaks at cluster 6 for *FOXA1* mutant (SY242CS-V5, H247Y-V5, S250F-V5 and F266L-V5) and WT-V5 in the absence (DMSO) or presence of estrogen (E2) at estrogen induced ER binding sites (from public dataset GSE59530 (Franco et al., 2015)). PC, Peak center.

(F) Venn diagram illustrating the overlap between cluster 6 peaks and estrogen induced ER binding sites (from public dataset GSE59530 (Franco et al., 2015)). DMSO, estrogen depletion; E2, upon estrogen stimulation.

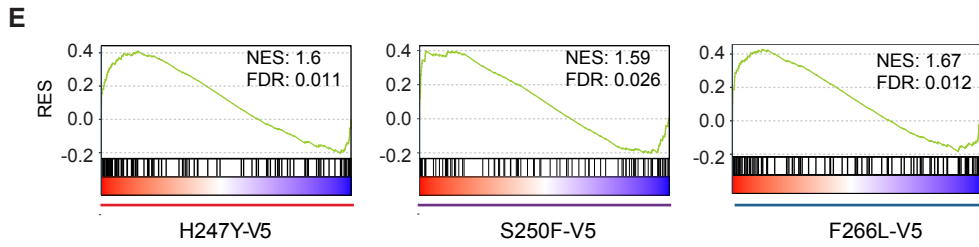
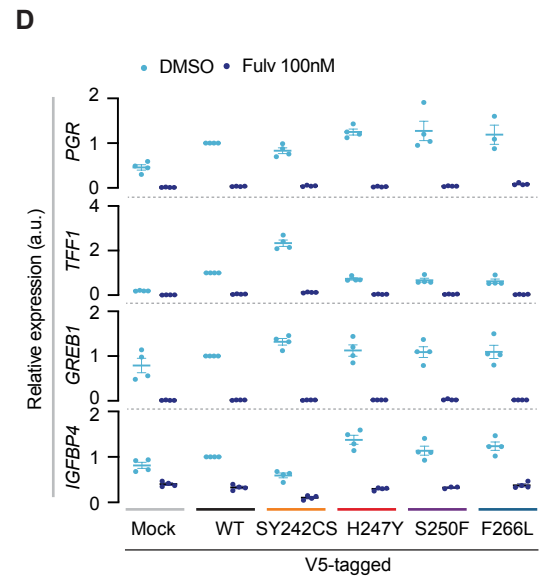
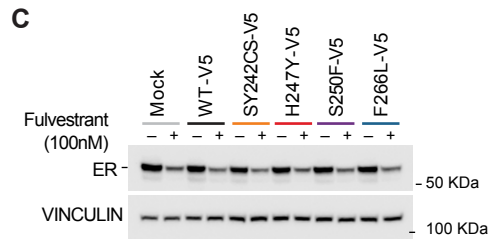
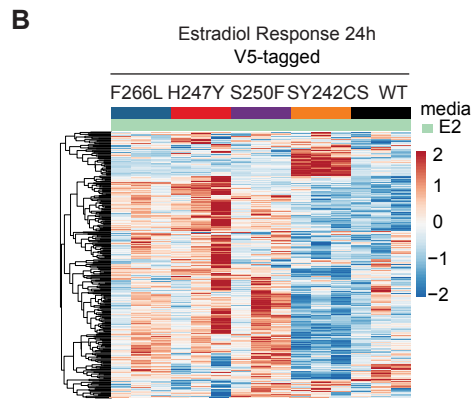
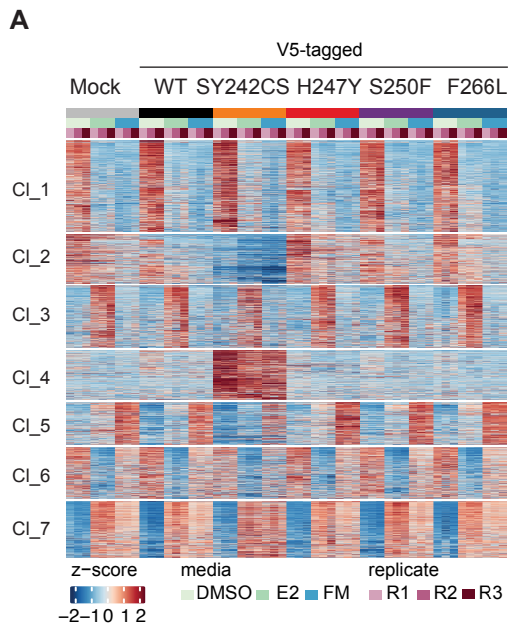


Figure S4. Related to Figure 4. FOXA1 mutants display enhanced ER-dependent estrogen response.

(A) Heatmap of k-means clustering of RNA-seq peaks from *FOXA1* mutant (SY242CS-V5, H247Y-V5, S250F-V5 and F266L-V5) and control (WT-V5, wild-type and Mock, empty vector) MCF7 cells, representing seven clusters (n=3 biological replicates).

(B) Heatmap showing expression level of genes from Gene Set Enrichment Analysis (GSEA) dataset 'Duterte Estradiol Response 24h Up' in RNA-seq from *FOXA1* Wing2 mutant cells (H247Y-V5, S250F-V5, F266L-V5 and SY242CS-V5) as compared to *FOXA1* WT-V5 cells.

(C-D) Impact of fulvestrant treatment (100nM, 72h) on ER protein levels (C, representative experiment is shown) and shared *FOXA1* and ER target gene expression (*IGFBP4*, *PGR*, *TFF1*, *GREB1*) in V5-tagged *FOXA1* variant (SY242CS, H247Y, S250F, F266L) expressing MCF7 cells (D) n=4 biological replicates.

(E) Gene Set Enrichment Analysis (GSEA) plot showing 'Y537S *ESR1* versus WT *ESR1* in HD' from Jeselsohn et al., 2018 enriched in RNA-seq from *FOXA1* Wing2 mutant cells (H247Y-V5, S250F-V5 and F266L-V5) as compared to *FOXA1* WT-V5 cells. RES, Running Enrichment Score, as indicated. FDR represents p adjusted value, calculated using the GSEA package. HD, Hormone depleted; RES, Running Enrichment Score.

DMSO, estrogen depletion; E2, upon estrogen stimulation; FM, in full media.

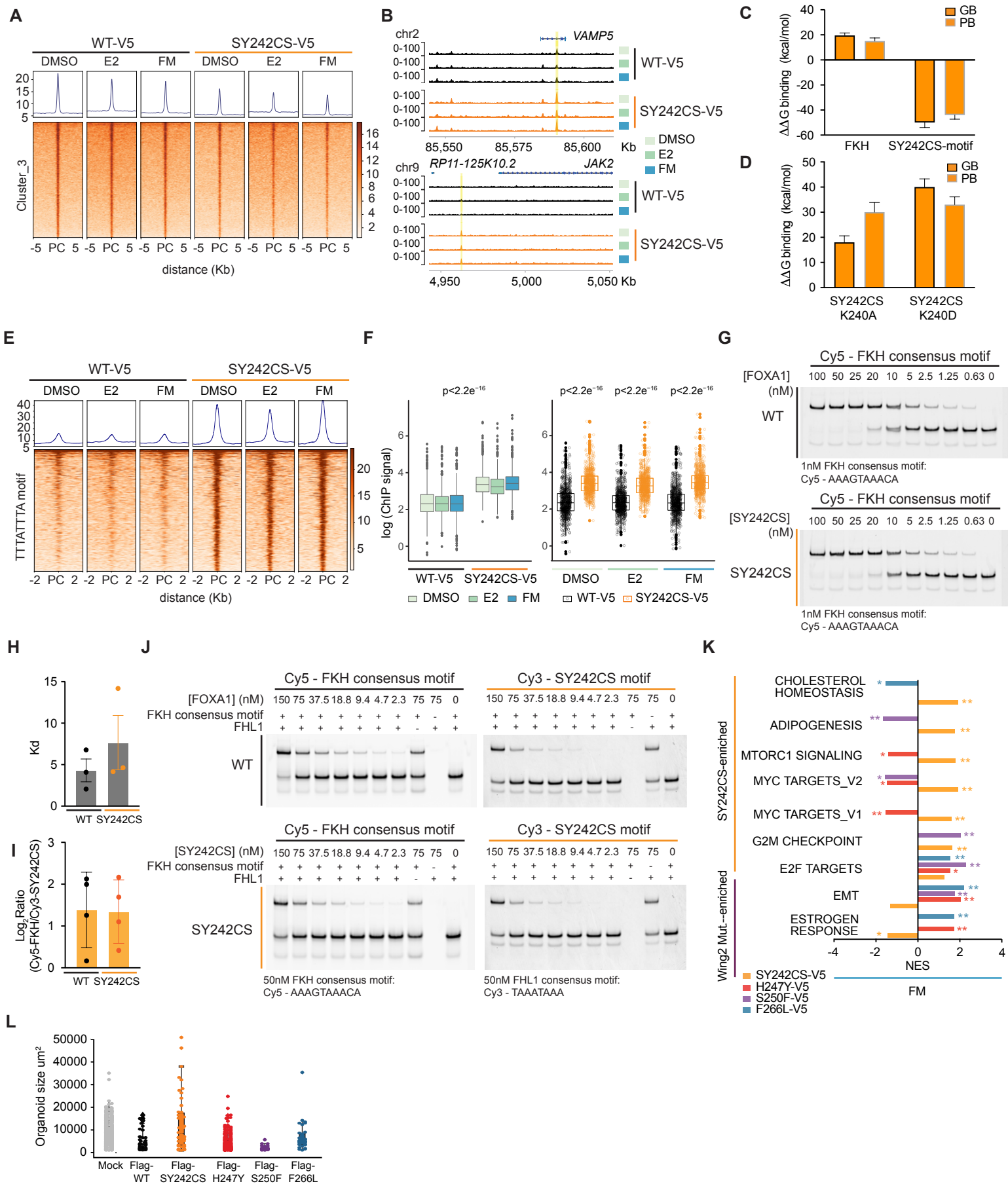


Figure S5. Related to Figure 5. FOXA1 SY242CS shows enrichment for alternative transcriptomic pathways.

(A) Tornado plot showing ChIP-seq peaks of FOXA1 cluster 3 in Figure 3B from MCF7 cells bearing either FOXA1 WT or SY242CS under the conditions indicated. PC, Peak center. Average of 2 biological replicates is represented. Average of 2 biological replicates is represented.

(B) ChIP-seq tracks of FOXA1 in either SY242CS-V5 or WT FOXA1 MCF7 cells at EFEMP1 and FST gene loci at chromosome 2 and 5 respectively, under media condition indicated.

(C-D) Quantification of binding free energy ($\Delta\Delta G$) of SY242CS to either FKH or SY242CS-specific motifs (C) and of SY242CS K240A or K240D mutants to SY242CS-specific motif, calculated using the Generalized Born (GB) and Poisson-Boltzmann (PB) formalisms averaged over the conformations of the complexes sampled during atomistic Molecular Dynamics (MD) simulations. Error bars equal SEM.

(E-F) Tornado plot (E, average of 2 biological replicates is represented) and quantification (F) of peaks that contain the SY242CS motif TTTATTTA in both WT or FOXA1 SY242CS mutant sites in all three medias. Anova test, $p < 2.2 \times 10^{-16}$.

(G-H) Representative gel image (G) and quantification (H) of EMSAs where FOXA1 WT and SY242CS peptides were titrated using a fluorescently labeled probe of the FOXA1 consensus forkhead (FKH) DNA element. The dissociation constant (Kd) was estimated by non-linear curve-fitting from three experiments. Error bars equal SEM.

(I-J) Representative gel image (I) and quantification (J) of competition ('picking') EMSA of FOXA1 WT and FOXA1 SY242CS peptides simultaneously incubated with the FKH consensus motif (AAAGTAAACA, Cy5) or the SY242CS-specific motif (TAAATAAA, Cy3). Relative proportions of protein-bound Cy3 and Cy5 probes in the same gel are determined using successive scans with Cy5 or Cy3 emission filters, respectively. Error bars equal STD.

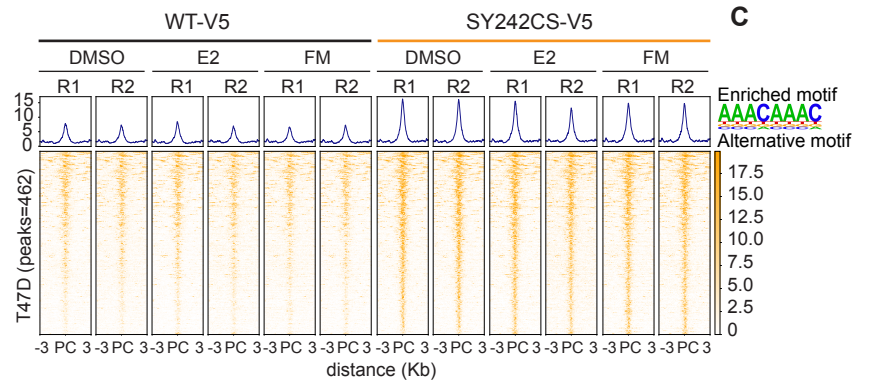
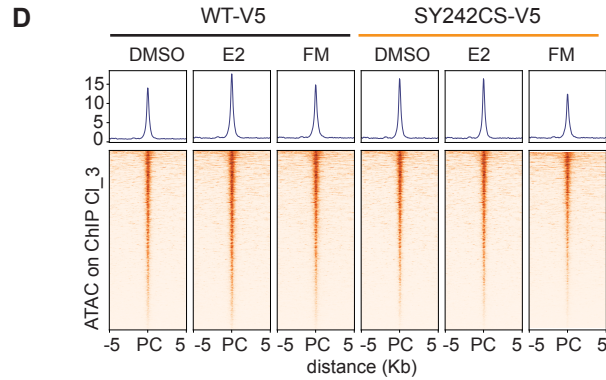
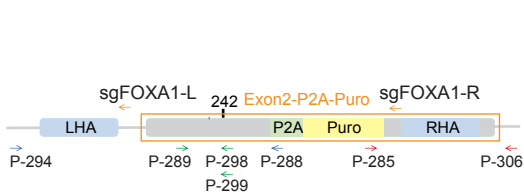
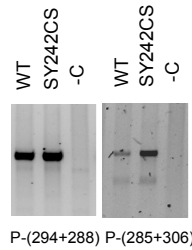
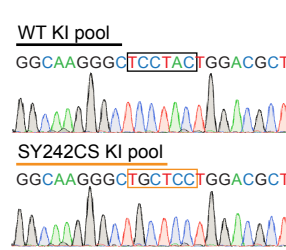
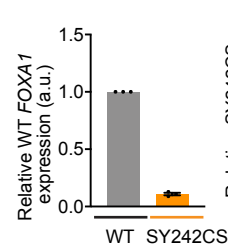
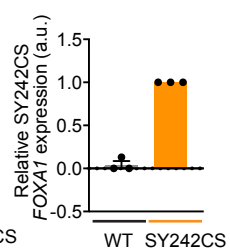
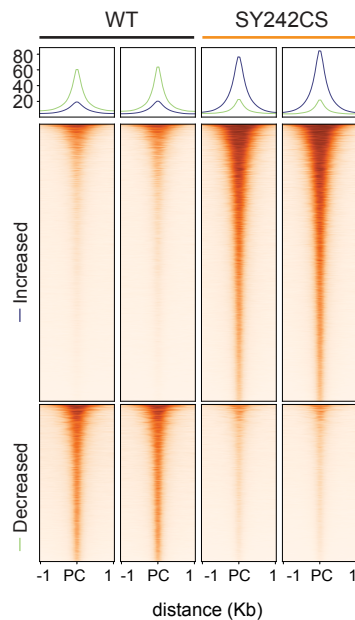
(K) Bar plot representing selected Hallmark datasets in FOXA1 SY242CS-V5 or Wing2 mutant MCF7 cells as compared to the FOXA1 WT-V5 control cells under the culture media condition indicated. NES, Normalized Enrichment Score. *, $\text{padj} < 0.05$; **, $\text{padj} < 0.01$; $\text{padj} < 0.001$.

(L) Quantification of organoid size (μm^2) measured seven days after seeding, from representative experiment. Values for sample size (indicated as dots) ($n=1$) Error bars equal STD.

DMSO, estrogen depletion; E2, upon estrogen stimulation; FM, in full media.

A

CI	Top enriched <i>de novo</i> motifs	T%	BG%	p-val
1	AGCAAACA FORKHEAD	55.19	28.71	1e-198
	CAGTTTGA MYB	10.74	4.44	1e-45
	CAGACTTIA SMAD	8.18	2.99	1e-42
2	TGACTCAI AP1	27.72	11.19	1e-201
	ACATTCCA TEAD	33.11	45.42	1e-189
	ITGTTTAC FORKHEAD	47.07	29.27	1e-138
3	ATGACTCA AP1	22.55	8.55	1e-130
	GIAAACA FORKHEAD	28.95	18.14	1e-51
	AAACCGTI GRHL1	27.37	21.05	1e-17
4	ATGACTCA AP1	36.14	13.04	1e-343
	CGSAACCF ETS	25.84	17.89	1e-59
	AACCGGTI GRHL1	21.90	13.87	1e-48
5	STGTTTAC FORKHEAD	45.67	26.73	1e-167
	CCCFAGG AP2gamma	36.68	25.77	1e-59
	CGCCACCF EGR	8.46	4.31	1e-34
6	TTTTATTA Alternative motif	43.84	17.60	1e-704
	AGGAATGI TEAD	25.97	17.95	1e-76
	CCCFAGG AP2gamma	40.66	31.52	1e-71
7	ATGACTCA AP1	31.60	11.26	1e-324
	AACCGGTI GRHL1	15.20	6.89	1e-91
	STATTTTC FORKHEAD	53.58	42.17	1e-58
8	TGTAAAF FORKHEAD	64.07	25.31	1e-281
	ATGACTCA AP1	23.54	8.54	1e-87
	CCGGTCC NUCLEAR RECEPTOR	2.12	0.46	1e-14

B**C****D****E****F****G****H****I****J****K**

Enriched motif
TTTTATTT
Alternative motif
($p=1e^{-3171}$)

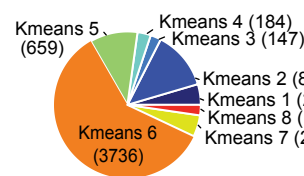
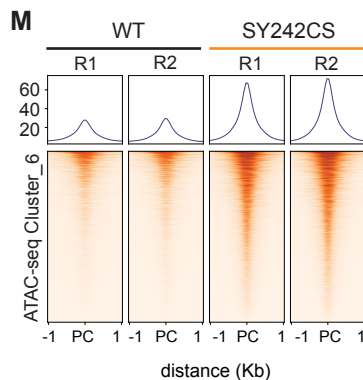
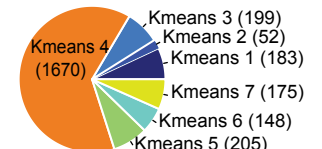
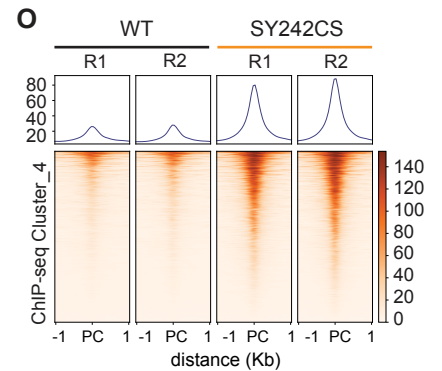
L**M****N****O**

Figure S6. Related to Figure 6. FOXA1 SY242CS gained binding sites correlate with increased accessibility and mRNA upregulation.

- (A) Table depicting top enriched Homer *de novo* motifs and the transcription factors associated with, per ATAC-seq cluster indicated. Fisher's exact test, p-value (p-val) as indicated. T%, percentage of target sites; BG%, background percentage; Cl, cluster.
- (B-C) Tornado plot (F) representing ATAC-seq peaks for FOXA1 SY242CS and WT T47D cells under the conditions indicated, and top enriched homer *de novo* motif for the represented peaks (G). PC, Peak center; R1, biological replicate one; R2, biological replicate two.
- (D) Tornado plot representing chromatin accessibility of peaks in ChIP-seq cluster 3 for FOXA1 SY242CS and WT MCF7 cells under the conditions indicated. PC, Peak center.
- (E) Schematic depicting the KI detection strategy of FOXA1 WT and SY242CS. Orange arrows: sgRNAs. Blue and red arrows: primers detecting left and right on-target insertion in genome. Green arrows: Primers detecting WT (P-289+P-299) or SY242CS FOXA1 (P-289+P298) cDNAs.
- (F) Agarose gel showing positive bands for left and right insertion in the genome for WT and SY242CS pooled MCF7 cells.
- (G) Sanger sequencing of the positive WT and SY242CS pooled MCF7 cells.
- (H-I) Relative WT (H) or SY242CS (I) expression. Error bars equal SEM.
- (J-K) Tornado plot showing increased and decreased differential chromatin accessibility peaks in WT or SY242CS pooled KI MCF7 cells. Also shown is the enriched motif for the SY242CS alternative motif TTTATTATTT ($p=1e^{-3171}$) by Fisher's Exact test ($n=2$ biological replicate).
- (L-M) Pie plot (L) and tornado plot (M) showing the distribution of overlapping peaks between the KI ATAC-seq peaks (SY242CS KI vs. WT KI) and the ATAC-seq cluster 6 obtained by overexpressing FOXA1 variants in MCF7 cells.
- (N-O) Pie plot (N) and tornado plot (O) showing the distribution of overlapping peaks between the KI ATAC-seq peaks (SY242CS KI vs. WT KI) and the ChIP-seq cluster 4 obtained by overexpressing FOXA1 variants in MCF7 cells.

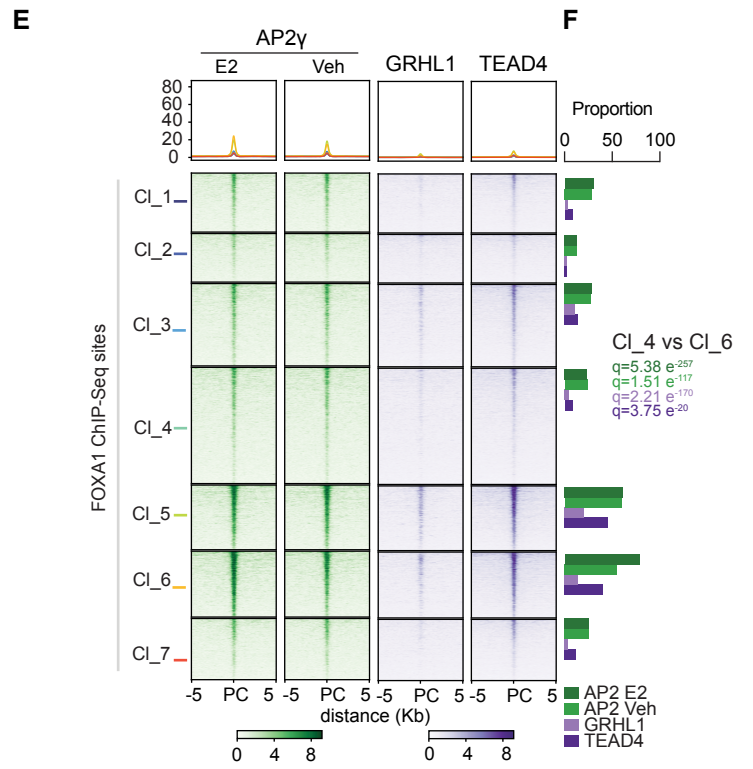
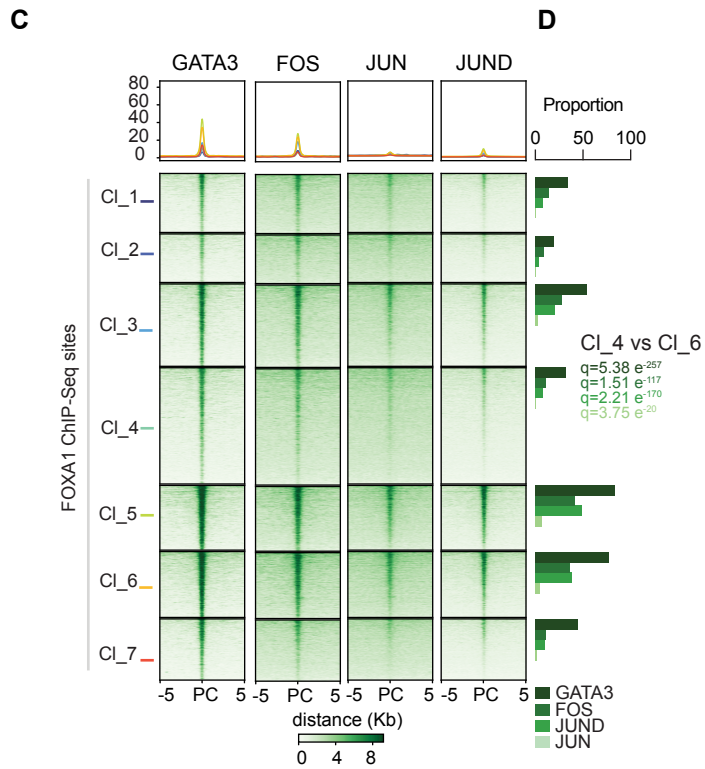
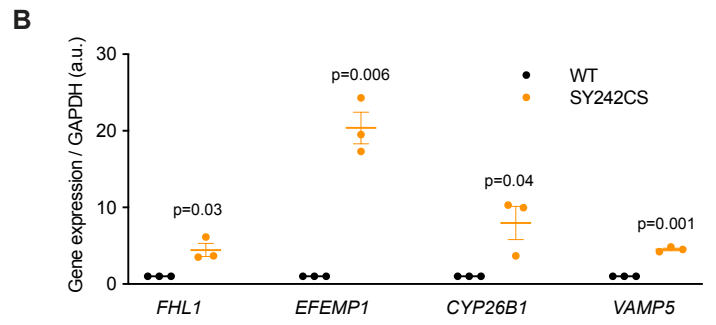
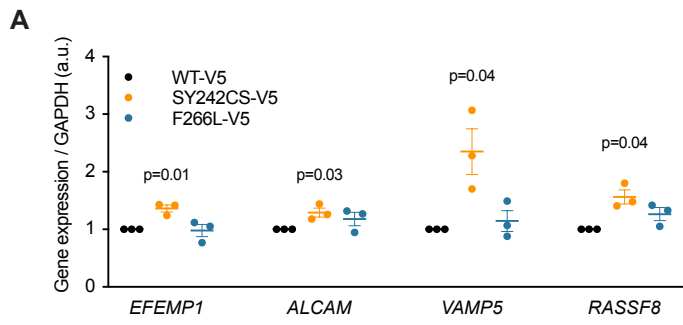


Figure S7. Related to Figure 7. FOXA1 cooperating factors show high chromatin occupancy at FOXA1 sites

(A) mRNA expression quantified by RT-QPCR of genes indicated in T47D cells expressing FOXA1 variants (SY242CS-V5 and F266L-V5) as compared to FOXA1 WT-V5 cells in FM.

(B) mRNA expression quantified by RT-QPCR of genes indicated in pooled KI MCF7 cells (WT and SY242CS FOXA1) in FM.

(C-D) Tornado plots (C) and bar plot (D) showing ChIP-seq peaks of public ChIP-seq data for transcription factors with enriched occupancy at FOXA1 ATAC-seq clusters in Figure 6A (GATA3 (ENCSR000BST) and AP1 (FOS, ENCSR569XNP; JUN, ENCSR176EXN; JUND, ENCSR000BSU) at FOXA1 ChIP-seq sites per cluster in Figure 3B indicated. Statistical test of cluster 4 vs cluster 6 as indicated.

(E-F) Tornado plots (E) and bar plot (F) showing ChIP-seq peaks of public ChIP-seq data for transcription factors with enriched occupancy at FOXA1 ATAC-seq clusters in Figure 6A (AP2gamma (GSE26741), GRHL1 (GSE140185) and TEAD (ENCSR000BUO)) at FOXA1 ChIP-seq sites per cluster in Figure 3B indicated. Statistical test of cluster 4 vs cluster 6 as indicated.

PC, Peak center; DMSO, estrogen depletion; E2, upon estrogen stimulation; Veh, vehicle treated.